Available online at www.sciencedirect.com
SCIENCE DIRECT®
Surface Science 554 (2004) 43–59
SURFACE SCIENCE
www.elsevier.com/locate/susc

Sum frequency generation and density functional studies of CO–H interaction and hydrogen bulk dissolution on Pd(1 1 1)

Günther Rupprechter [a,*], Matthias Morkel [a], Hans-Joachim Freund [a], Robin Hirschl [b]

[a] *Department of Chemical Physics, Fritz-Haber-Institut der Max-Planck-Gesellschaft, Faradayweg 4-6, Berlin D-14195, Germany*
[b] *Center for Computational Materials Science, Institute of Materials Physics, University of Vienna, Sensengasse 8/12, Vienna A-1090, Austria*

Received 14 November 2003; accepted for publication 4 February 2004

Abstract

CO–H interaction and H bulk dissolution on Pd(1 1 1) were studied by sum frequency generation (SFG) vibrational spectroscopy and density functional theory (DFT). The theoretical findings are particularly important to rationalize the experimentally observed mutual site blocking of CO and H and the effect of H dissolution on coadsorbate structures. Dissociative hydrogen adsorption on CO-precovered Pd(1 1 1) is impeded due to an activation barrier of ~2.5 eV for a CO coverage of 0.75 ML, an effect which is maintained down to 0.33 ML CO. Preadsorbed hydrogen prevented CO adsorption at 100 K, while hydrogen was replaced from the surface by CO above 125 K. The temperature-dependent site blocking of hydrogen originates from the onset of hydrogen diffusion into the Pd bulk around 125 K, as shown by SFG and theoretical calculations using various approaches. When Pd(1 1 1) was exposed to 1:1 CO/H_2 mixtures at 100 K, on-top CO was absent in the SFG spectra although hydrogen occupies only threefold hollow sites on Pd(1 1 1). DFT attributes the absence of on-top CO to H atoms diffusing between hollow sites via bridge sites, thereby destabilizing neighboring on-top CO molecules. According to the calculations, the stretching frequency of bridge-bonded CO with a neighboring bridge-bonded hydrogen atom is redshifted by 16 cm^{-1} when compared to bridging CO on the clean surface. Implications of the observed effects on hydrogenation reactions are discussed and compared to the C_2H_4–H coadsorption system.

Keywords: Sum frequency generation; Density functional calculations; Palladium; Carbon monoxide; Hydrogen molecule; Alkenes; Low index single crystal surfaces; Catalysis; Vibrations of adsorbed molecules

1. Introduction

The interaction of CO and hydrogen on transition metals is of both fundamental and technical interest, because the coadsorption of H with another molecule is an important initial step in

* Corresponding author. Tel.: +49-30-8413-4132; fax: +49-30-8413-4105.
E-mail address: rupprechter@fhi-berlin.mpg.de (G. Rupprechter).

0039-6028/$ - see front matter © 2004 Elsevier B.V. All rights reserved.
doi:10.1016/j.susc.2004.02.008

catalytic hydrogenation. On Pd surfaces, the seemingly "simple" CO/H system becomes complex due to the large number of well-ordered CO structures on Pd single crystals ([1,2] and references therein) and due the various states of adsorbed and absorbed (dissolved) hydrogen (see e.g. [3,4]). It is not surprising, though, that some controversy still exists on the exact mechanism of CO hydrogenation on Pd catalysts [5,6]. Many surface-analytical studies were devoted to the individual adsorption of CO *or* hydrogen on Pd single crystal surfaces while only a limited number of coadsorption studies exists. Still, several effects were reported, e.g. blocking of hydrogen adsorption by CO [7–9], formation of subsurface H and H absorption [8,10–13], CO-induced hydrogen dissolution in the Pd bulk [9,14,15], differences in catalytic activity of surface and bulk H [16,17], etc. Recent scanning tunneling microscopy (STM) studies by the Salmeron group allowed to image a hydrogen-induced compression of CO and oxygen islands on Pd(1 1 1), as well as H dissociation and dissolution [18–21]. However, the coadsorption studies were mostly carried out by sequential dosing (dosing e.g. H_2 first, CO after) while *a mixture* of reactant molecules interacts with the catalyst during a reaction.

Here we describe both types of gas exposure (sequential dosing and co-dosing), and it is shown that different adsorption site occupancies are obtained. Sum frequency generation (SFG) vibrational spectroscopy was employed to monitor CO–H intermolecular interactions and H bulk dissolution. Part of the spectroscopic results were presented earlier [22,23] but the previous interpretation was based on comparisons with results obtained by other *experimental* techniques, e.g. temperature-programmed desorption (TPD), low-energy electron diffraction (LEED), infrared reflection absorption spectroscopy (IRAS), STM, etc. In this article, density functional calculations are employed to provide a theoretical basis for a better understanding of the mutual site blocking of CO and hydrogen and of hydrogen bulk dissolution. We also discuss implications of the observed effects on other reactions involving hydrogen, e.g. C_2H_4 hydrogenation.

2. Methods

2.1. Experimental

Experiments were carried out in a UHV surface analysis system combined with an SFG-compatible UHV-high-pressure cell, described in more detail in [1,24]. The UHV section (base pressure 1×10^{-10} mbar) is equipped with LEED, TPD and Auger electron spectroscopy (AES). Following preparation and characterization, the sample is transferred under UHV to the SFG cell, which has two CaF_2 windows for optical spectroscopy. For a description of the most important aspects of SFG theory (with respect to signal intensity, lineshape, selection rules) and the laser setup we refer to [1,25] and references therein. Very briefly, picosecond laser pulses at a tunable infrared frequency ω_{IR} and at a fixed visible frequency ω_{VIS} are spatially and temporally overlapped on the adsorbate/Pd(1 1 1) surface. When the IR frequency coincides with a vibrational resonance of the adsorbate, an SFG signal is generated at the sum frequency ($\omega_{SFG} = \omega_{IR} + \omega_{vis}$). Thus, plotting the SFG intensity vs. the IR wavenumber results in a vibrational spectrum. TPD spectra were recorded with a heating rate of 1 K/s with CO coverages being determined by integration of TPD areas, using the ($2\times$ 2) 0.75 ML CO saturation structure as reference. To avoid "non-equilibrium" structures [22], some exposures were carried out by cooling Pd(1 1 1) in the respective gas.

The Pd(1 1 1) surface was prepared by sequences of flashing to 1250 K, Ar^+ bombardment (700 V at 5×10^{-6} mbar, 5 μA current), annealing to 1250 K and oxidation between 1200 and 600 K in 5×10^{-7} mbar O_2, followed by a final flash to 1200 K. Its surface structure and cleanliness were confirmed by LEED, AES and CO-TDS. To remove Ni- and Fe-carbonyl impurities, CO (purity $\geqslant$ 99.997%) was passed over a carbonyl absorber cartridge and then introduced via a cold trap filled with liquid nitrogen. Hydrogen (purity $\geqslant$ 99.99990) and ethylene (purity $\geqslant$ 99.95) were cleaned using a cold trap. For UHV exposures the pressure indicated by the ionization gauge was corrected by the sensitivity factors for CO (1.0), H_2 (0.44) and C_2H_4 ($\sim$2).

When gas mixtures were used, CO and H_2 were premixed in a glass bulb at mbar pressures using a baratron gauge.

2.2. Computational

Density functional theory (DFT) calculations were performed using the plane-wave based Vienna ab initio simulation package (VASP) [26,27] to solve the single-particle Kohn–Sham equations. Generalized gradient corrections (GGA) as proposed by Perdew and Wang (PW91) [28] were applied to improve the local density approximation. Adsorption energies of CO and H_2 are generally overestimated using the PW91 functional. Another GGA approximation, the revised Perdew–Burke–Ernzerhof functional (RPBE) [29] yields adsorption energies which better agree with experiments for CO but cannot be applied for dissociative H_2 adsorption. Calculations including hydrogen were therefore carried out using the PW91 functional. Brillouin-zone sampling was performed on Monkhorst–Pack special points [30], integrated utilizing a generalized Gaussian smearing. The plane-wave cutoff was 400 eV for all calculations, convergence with respect to the energy cutoff and the number of k-points was confirmed.

Electron–ion interactions are described by the projector-augmented-wave (PAW) method of Blöchl [31] in the formulation of Kresse and Joubert [32]. This essentially all-electron method improves the description of transition metals compared to the use of pseudopotentials.

The surfaces and adsorbates were simulated in supercells with periodic boundary conditions consisting of four layers of substrate and four layers of vacuum. Unless otherwise stated below the cells had a p(2×2) geometry leading to an adsorbate coverage of 0.25 ML. Ionic relaxation of the adsorbate and the topmost surface layers is performed after determining the Hellmann–Feynman forces [33] acting on the atoms. In the molecular dynamics calculations a micro-canonical ensemble is simulated for simplicity. Vibrational frequencies are calculated by numerical approximation of the Hessian matrix using finite differences and determination of its eigenvalues. The coupling of adsorbate vibrations to surface phonons is neglected. This does not introduce significant errors since the adsorbate frequencies of interest are orders of magnitude higher than the surface phonon frequencies.

3. Results and discussion

3.1. CO adsorption and H_2 adsorption on Pd(1 1 1)

3.1.1. CO adsorption

CO adsorption on Pd(1 1 1) has been the subject of many experimental studies using a variety of techniques, for instance TPD [34–36], LEED [37,38], IRAS [39–41], STM [18,42], X-ray photoelectron spectroscopy (XPS) [43,44], SFG [1,2,45,46] and others. At least 17 ordered structures were observed, the most important being a $(\sqrt{3}\times\sqrt{3})R30°$-1CO at 0.33 ML, a c(4×2)-2CO at 0.5 ML, a $(4\sqrt{3}\times 8)$rect at 0.63 ML and a (2×2)-3CO at 0.75 ML (1 ML equals the density of Pd atoms in the (1 1 1) plane; 1.53×10^{15} cm^{-2}).

Each adsorbate structure exhibits a characteristic vibrational spectrum and LEED pattern (see e.g.) [1,22,47]. CO first adsorbs in threefold hollow sites with a stretching frequency around 1850 cm^{-1} at 0.33 ML. At 0.5 ML, a peak at 1920 cm^{-1} is observed and two types of c(4×2) structures coexist. One with CO in fcc and hcp threefold hollow sites and one with bridge bonded CO [18,40,43,48–50]. Between 0.5 and 0.6 ML the CO peak continuously shifts to higher wavenumbers. Above $\theta = 0.6$, CO is preferentially bridge bonded (~1955 cm^{-1}) with a smaller amount of linear (on-top) CO at 2075–2090 cm^{-1} whose intensity is very sensitive to coverage. If the coverage is further increased, the adsorbate layer rearranges finally leading to a (2×2) saturation structure ($\theta = 0.75$; Fig. 1(a)) including fcc and hcp hollow (1899 cm^{-1}) and on-top bonded CO (2108 cm^{-1}) [1,41].

An extensive ab initio database of CO chemisorption energies including Pd(1 1 1) was reported by Hammer et al. [51]. Sautet and coworkers have carried out comprehensive DFT investigations of CO/Pd(1 1 1), aiming at the interpretation of stretching frequencies [49] and of STM images [42].

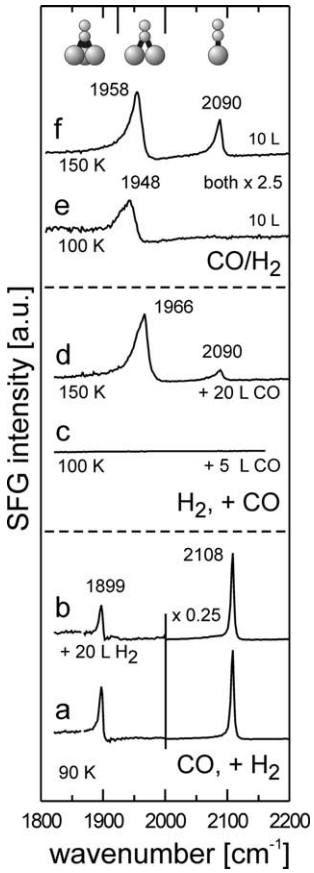

Fig. 1. SFG spectra of CO–H coadsorbate structures on Pd(1 1 1) demonstrating the difference between sequential dosing of CO and H_2 (a–d) and CO/H_2 mixtures (e,f). After saturating Pd(1 1 1) with ~1000 L CO by cooling in 3×10^{-6} mbar CO from 300 to 90 K (a), 20 L hydrogen were dosed at 90 K (b). After cooling Pd(1 1 1) in 1×10^{-7} mbar H_2 from 300 to 100 K (~100 L), 5 L CO were dosed (c). After cooling Pd(1 1 1) in 1×10^{-7} mbar H_2 from 300 to 150 K (~50 L), 20 L CO were dosed (d). Exposure of Pd(1 1 1) to 10 L of a 1:1 CO/H_2 mixture at 100 K (e) and 150 K (f).

In contrast to Pt(1 1 1) where experimental and DFT disagree about the preferred adsorption site [52,53], on Pd(1 1 1) DFT correctly establishes the threefold hollow site as the most favorable site for CO adsorption, proceeding molecularly, and in an upright geometry with the C atom pointing towards the surface. At low coverage the two threefold hollow sites (fcc and hcp) are very close in adsorption energy, at $\theta = 0.33$ the fcc site is slightly preferred by ~30 meV [42,50,54]. The adsorption energy at the fcc hollow site is 2.02 eV at 0.33 ML when the PW91 exchange-correlation functional is used (1.99 eV for hcp). This is far above the adsorption energy determined from TDS measurements, being 1.48–1.54 eV [34,36,55]. The RPBE exchange-correlation functional, which was specifically designed to better reproduce adsorption energies yields an adsorption energy of 1.63 eV (but it fails completely for H_2 adsorption). Similar values were reported for CO adsorption on Pd clusters ($\geqslant 80$ atoms) exhibiting (1 1 1) facets [56,57]. Ab initio calculations (using embedding theory) by Klüner et al. [58,59] yielded an adsorption energy of 1.42 eV for CO in an fcc hollow site (0.125 ML coverage).

The adsorption energy difference between the threefold hollow sites and the twofold bridge sites on Pd(1 1 1), i.e. the diffusion barrier for horizontal diffusion at low coverage, does not depend considerably on the functional used and is about 0.15 eV [54]. On-top adsorption at 0.33 ML (1.42 eV) is 0.6 eV less stable than fcc adsorption (2.02 eV). Increasing the CO coverage from 0.33 to 0.75 ML further reduces the adsorption energy per CO molecule by 25%, indicating a strong inter-adsorbate repulsion. This repulsion hinders adsorbed CO molecules to come close to each other, largely suppressing diffusion at high coverage.

3.1.2. H_2 adsorption and dissolution

Studies of hydrogen adsorption and absorption on Pd single crystals have identified different types of hydrogen species including surface hydrogen, subsurface hydrogen (situated between the first and second substrate layers), near-surface hydrides and bulk hydrogen forming a homogeneous solution of H in the bulk metal lattice (cf. [3,4]). The relative abundance of the different H-species depends on the adsorption temperature and the exposure conditions (pressure/time). When Pd(1 1 1) was cooled from 300 to 100 K in 1×10^{-7} mbar H_2 (equal to ~100 L; 1 L amounts 10^{-6} Torr s), adsorbed hydrogen could not be detected by SFG (similar to Fig. 1(c)) because the Pd–H stretch vibration (~60 meV) [60] is outside the frequency range of our instrument. However, in agreement with previous reports H_2-TDS exhibits a single desorption peak with a maximum at

295 K, originating from the recombinative desorption of surface hydrogen and of hydrogen from subsurface and bulk sites ([8,61,62], cf. Fig. 3(a)).

Interesting values that can be provided by DFT calculations are (i) the barrier for dissociative hydrogen adsorption, (ii) the adsorption energies in surface and subsurface sites and (iii) the barriers for horizontal as well as vertical H diffusion.

(i) The dissociative adsorption of H_2 on Pd(1 1 1) was previously studied by total energy calculations using VASP [63]. Six possible dissociation pathways/sites were investigated that were either non-activated or slightly activated (involving different adsorption geometries of the H atoms in the H_2 molecule adsorbing in fcc, hcp, bridge and top sites) and only the top–top path (both H atoms adsorb on on-top sites) did not lead to a stable dissociation state (for illustrations see [63]). It was concluded that dissociative H_2 adsorption is a non-activated process, i.e. it occurs spontaneously even at $T = 0$ K.

(ii) On Pd(1 1 1), atomic hydrogen preferably adsorbs in the threefold hollow site. We have calculated the adsorption energy per hydrogen atom to be 0.59 eV in fcc hollows for a full monolayer ($\theta = 1$), increasing only slightly for lower coverages (0.61 eV for $\theta = 0.33$). Adsorption energy differences to (the less stable) bridge and top sites were previously determined to be 0.19 and 0.55 eV, respectively [64]. For a full monolayer of hydrogen atoms in octahedral subsurface sites (above a third-layer atom) the adsorption energy per atom is 0.23 eV. Zero point energies are not considered. They would not, however, change the qualitative picture.

(iii) Diffusion barriers were calculated for horizontal diffusion from fcc to hcp hollow sites via a bridge site ($E_{diff} = 0.19$ eV at 1 ML [64,65]) and for vertical diffusion from an fcc hollow to an underlying octahedral subsurface site ($E_{diff} = 0.40$ eV at 0.25 ML, this work). While the former assumed the bridge adsorption position as transition state, the latter was obtained applying the nudged elastic band method [66] with the two uppermost substrate layers allowed to relax. Previously Lynch et al. have published activation barriers from embedded atom method (EAM) calculations for horizontal and vertical diffusion to be 0.20 and 0.07 eV, respectively [67]. However, in light of recent experimental observations (rapid horizontal H diffusion already at 25 K, vertical diffusion around 200 K [19,20]) and of calculations on the even more open Rh(1 0 0) surface [68] the higher value seems more appropriate.

3.2. H adsorption on CO-precovered Pd(1 1 1)

The inhibition of H adsorption by preadsorbed CO has been repeatedly observed experimentally [7–9] but the SFG spectra are shown for completeness in Fig. 1(a) and (b) (for corresponding LEED and TDS measurements see e.g. [9,23]). After saturating Pd(1 1 1) with ~1000 L CO (by cooling in 3×10^{-6} mbar CO from 300 to 90 K), SFG indicated the formation of a well-ordered (2×2; 0.75 ML) hollow/on-top-CO structure with narrow peaks at 1899 and 2108 cm^{-1} (Fig. 1(a)). After dosing 20 L H_2 at 90 K on the CO-precovered Pd(1 1 1) surface, no changes were observed by SFG (Fig. 1(b)) and also TDS did not show any H_2 desorption. On clean Pd(1 1 1) less than 1 L hydrogen would be sufficient at 90 K to produce a near monolayer hydrogen coverage [9,61]). Since no hydrogen adsorbed on the CO-precovered surface, the sites for dissociative hydrogen adsorption were apparently blocked by CO.

Although the 0.75 ML CO layer is quite dense, the suppression of H adsorption cannot be explained by a mere physical blocking of sites required for dissociative hydrogen adsorption. As mentioned, Dong and Hafner [63] studied six possible non-activated dissociation pathways/sites involving various adsorption geometries of the H_2 molecule. Even though the (2×2) structure has 3 CO molecules in the unit cell (2 hollow, 1 on-top), in a purely geometric picture several of these adsorption configurations would be still accessible. Consequently, a geometric picture does not apply and preadsorbed CO rather modifies the electronic structure of the adsorbate/substrate system, e.g. by increasing the barrier for hydrogen adsorption.

This was modeled by density functional calculations for the (2×2)-3CO structure using a 2×2 supercell. Fig. 2(a) depicts the supercell and three CO molecules adsorbed in top, fcc, and hcp hollow sites, respectively. The total CO adsorption energy per supercell is 4.48 eV, i.e. 1.08 eV (19%) less than the sum of three isolated CO molecules in the respective positions (at 0.14 ML, E_{ad}: 1.44 eV (top), 2.05 eV (hcp), and 2.07 eV (fcc) [54]).

After having established the CO-covered Pd(1 1 1) surface, the possibility of subsequent hydrogen adsorption was investigated. In this context it is interesting to note the recent finding of Mitsui et al. that on clean Pd(1 1 1) hydrogen needs at least three neighboring empty sites to adsorb dissociatively [20,69]. As mentioned, dissociative hydrogen adsorption on clean Pd(1 1 1) is a non-activated process. H_2 approaches the surface in a vertical (perpendicular) configuration above a substrate atom, tilts to a horizontal (parallel) configuration around 2.5 Å above the surface and then adsorbs in two neighboring threefold hollow sites. First, we have investigated a possible final state for the dissociative adsorption of H_2 on CO-precovered Pd(1 1 1). The positions of the H atoms are indicated in Fig. 2(a) by crosses. All adsorbate molecules (as well as the uppermost two layers of the substrate) were allowed to relax. The adsorption of two H atoms in a unit cell of (2×2)-3CO structure was found to be endothermic by 1.40 eV. There is a substantial repulsion between CO and H, i.e. the CO molecules are pushed away from the hydrogen atoms and vice versa, which may explain the experimentally observed

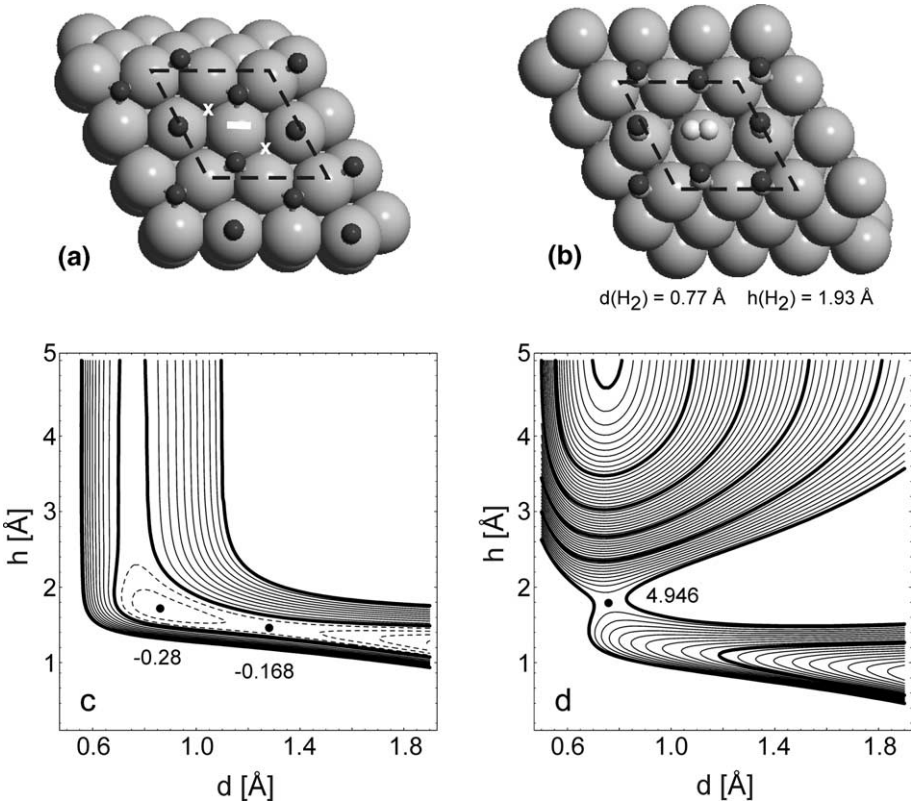

Fig. 2. (a) The (2×2)-3CO structure on Pd(1 1 1). The white line indicates the position and orientation of the adsorbing H_2, "×" marks the final H adsorption positions. (b) Transition state along the dissociative adsorption pathway of H_2 above CO-precovered Pd(1 1 1). The initially fcc hollow adsorbed CO molecules are pushed towards bridge positions. (c,d) Elbow plots of the vertical approach of a H_2 molecule in bridge-top-bridge configuration above clean Pd(1 1 1) (c) and CO precovered ($\Theta = 0.75$ ML) Pd(1 1 1) (d). All coordinates besides h and d of the molecule were kept fixed.

phase separation of CO and H [18,70]. All threefold hollow positions are equivalent in lying next to a hollow site occupied by a CO molecule so that a diffusion of a H atom to another hollow adsorption site does not improve the energetics as long as CO and H do not segregate into separate islands.

A practical means to visualize the potential energy surface (PES) of a H_2 molecule approaching the Pd surface is the so-called "elbow plot". The potential energy is scanned along two (height and H–H distance) of the six degrees of freedom of the molecule with all other degrees of freedom (two angles and the horizontal position of the adsorbate) kept fixed. Fig. 2(c) shows the PES for a vertical bridge-top-bridge configuration (indicated in Fig. 2(a)) of the H_2 molecule above a clean Pd(1 1 1) surface ("btb" as described in [63]). It is clearly seen that the whole minimum energy path (MEP) is exothermic. However, on the CO-covered surface (Fig. 2(d)) the picture fully changes. For the adsorption geometry chosen, the transition state now lies almost 5 eV above the energy of the desorbed H_2 molecule, i.e. the MEP is strongly endothermic. This is, however, without the CO molecules allowed to relax. The transition state in the reaction with all adsorbates allowed to relax, i.e. the saddle-point in a higher dimensional PES, lies 2.56 eV above the initial state. The atomic configuration in this state is shown in Fig. 2(b). From these results we conclude that it is extremely unlikely that hydrogen adsorbs dissociatively on a CO-precovered Pd(1 1 1) surface, in agreement with the generally accepted experimental finding. Hydrogen is most likely already reflected by the CO-layer (due to strong Pauli-repulsion, see Fig. 2(d)) and does not reach the Pd-surface.

Experimental studies on Pd(1 1 1) precovered with lower amounts of CO have shown that the inhibition of H adsorption is maintained down to a CO coverage of 0.33 ML [9]. It is reasonable to assume that a high adsorption activation barrier also exists under these conditions. Below 0.33 ML (total) CO coverage, H can adsorb but the total CO coverage (as determined by TPD) is somewhat misleading in this case. Since the CO molecules arrange into $(\sqrt{3}\times\sqrt{3})R30^\circ$ structures (local coverage 0.33 ML) already at total coverages well below 0.33 ML [18,40], free Pd areas exist between the CO islands allowing for H adsorption. Strong site blocking exceeding purely geometric effects was also reported for S [71–73], C, O, P and Cl [74,75].

3.3. CO adsorption on H-precovered Pd(1 1 1)

When hydrogen adsorption was followed by CO exposure, the resulting adsorbate structures were strongly temperature-dependent (Fig. 1(c) and (d)). The Pd(1 1 1) surface was first cooled from 300 to 100 K in 1×10^{-7} mbar H_2 ($\sim$100 L), leading to H adsorption in surface and subsurface/bulk Pd sites. No resonance was observed by SFG, as described in Section 3.1. Fig. 1(c) shows the SFG spectrum acquired after exposing 5 L CO on H-precovered Pd(1 1 1) at 100 K. SFG did still not detect any CO resonances and also CO-TDS and LEED did not indicate CO adsorption. Apparently, H-preexposure at 100 K led to a strong inhibition of CO adsorption [8,76]. On clean Pd(1 1 1) an exposure of 2 L CO would be sufficient to produce a coverage of at least 0.6 ML CO.

In order to model CO adsorption on H-precovered Pd(1 1 1) by DFT, a full monolayer of H atoms in fcc hollow sites was assumed (in agreement with experiments [20,21,62]). The only exothermic adsorption position for CO under these circumstances was the on-top site but the calculated adsorption energy was very small, i.e. 140 meV without consideration of the zero point energy (ZPE). Beside the metal-CO and the horizontal vibrations of the adsorbate, translational and rotational entropy has to be taken into account for a full picture of the free energy. Therefore, since we know that the PW91 GGA even overestimates CO adsorption energies, we conclude that CO is unstable on H-precovered Pd(1 1 1) at 100 K.

However, when the H-precovered surface was exposed to 20 L CO at 150 K (Fig. 1(d)), a different structure was observed, including bridge (1966 cm^{-1}) and on-top (2090 cm^{-1}) bonded CO, typical of a $\sim$0.65 ML CO coverage [1,2]. The SFG spectrum is identical to a corresponding

measurement without preadsorbed hydrogen suggesting that surface hydrogen was absent, i.e. there was a complete removal of surface hydrogen by CO. This was further supported by TPD. Fig. 3(c) and (d) display TPD traces obtained after adsorbing 20 L CO on a H-precovered surface at 150 K. CO-TPD (Fig. 3(d)) indicates a ~0.65 ML CO coverage and is nearly identical to a corresponding measurement without preadsorbed H (Fig. 3(b)). Furthermore, in H_2-TPD (Fig. 3(c)) the area of the H_2 desorption peak remained unchanged when compared to pure H_2 adsorption (Fig. 3(a)) ruling out significant hydrogen desorption but the peak was shifted from 295 to 375 K and now had a pronounced high temperature tailing, typical of diffusion-controlled desorption kinetics [7,8,13, 61,77]. This indicates that at 150 K CO removes/replaces hydrogen from the surface which most likely moves to the Pd bulk. Calculations supporting the assumption of H bulk diffusion at 150 K will be presented in Section 3.5.

3.4. Adsorption of $CO–H_2$ mixtures

In order to probe the interaction of a reactant *mixture* with a catalyst surface, we have premixed CO and H_2 in a glass bulb and co-dosed them to Pd(1 1 1). Adsorbate layers including both CO and H could thus be produced in which the CO island structure was strongly modified by hydrogen. When 10 L of a 1:1 CO/H_2 mixture were dosed at 100 K (Fig. 1(e)), the SFG spectrum exhibited a single peak at 1948 cm^{-1} (bridge bonded CO) while *on-top CO was absent*. CO-TDS indicated that the CO coverage was limited to ~0.55 ML, while H_2-TDS showed a hydrogen coverage of ~0.1 ML. This indicates a strong interaction of CO and H because an exposure of ~5 L pure CO under these conditions would produce a dense CO structure with $\theta \sim 0.7$, including a strong on-top peak in SFG as shown in Fig. 1(a).

Apparently, a CO/H_2 mixture leads to a "new" adsorbate structure, limited to ~0.55 ML CO and

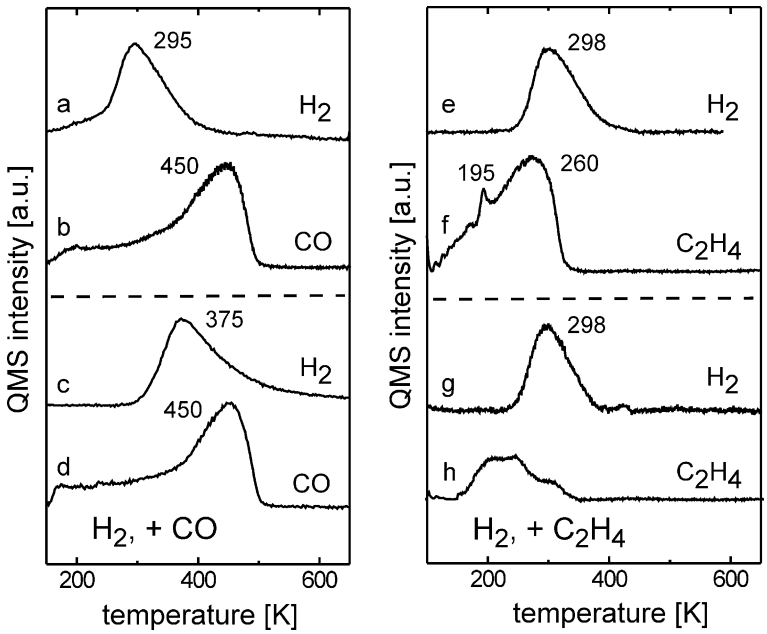

Fig. 3. Thermal desorption spectra of hydrogen (mass 2), CO (mass 28) and C_2H_4 (mass 27) on Pd(1 1 1). Desorption spectra of the individual components are shown in (a,b,e,f), those of coadsorption in (c,d,g,h). Exposures were as follows: (a) cooling in 1×10^{-7} mbar H_2 between 300 and 150 K (≈50 L); (b) cooling in 3×10^{-6} mbar CO from 300 to 190 K (≈500 L), producing a ~0.65 ML CO coverage; (c) and (d) display the desorption traces obtained after exposing Pd(1 1 1) to ~50 L H_2 and subsequently to 20 L CO at 150 K; (e) 1 L H_2 at 95 K; (f) 1 L C_2H_4 at 95 K; (g) and (h) display the desorption traces after exposing Pd(1 1 1) to 1 L H_2 and subsequently to 1 L C_2H_4 at 95 K.

without on-top bonded CO. This is in agreement with STM results by Rose et al. [18] who reported that when CO and H coexisted on Pd(1 1 1), hydrogen was able to compress a $(\sqrt{3} \times \sqrt{3})R30°$ CO layer into a c(4×2) 0.5 ML structure but not to a (2×2) (0.75 ML). The absence of on-top CO indicates that hydrogen either prevents CO adsorption on top-sites at all, or at least promotes an adsorbate structure that does not include on-top CO (see below). A "destabilisation" of on-top CO (and its shift to bridge sites) upon hydrogen adsorption has also been reported for Pt(1 1 1) [78], Pt(3 3 5) [79], Ni(1 1 1) [80] and Ni(1 0 0) [81].

Such a strong CO–H interaction may point to an intermixed CO–H layer. However, repulsive interactions between CO and H were frequently observed ([19,70]) which lead to separate CO and H islands. Therefore, it is difficult to understand how CO–H interaction influences the adsorbate structure *within* the CO islands (i.e. why is there no on-top CO within the CO islands?). One way to explain this behavior is that the CO–H interaction at the island boundaries is "passed on" to inner island regions. In fact, STM studies by the Salmeron group [18,19] have shown that the hydrogen-induced compression of CO (or oxygen) structures started at the island edges and proceeded towards the island center.

Based on these considerations, the interaction of neighboring CO and H atoms, simulating the situation at the domain boundaries, was further studied by DFT calculations. The first question to answer was which adsorption sites will be populated by CO and H. We used the (2×2)-3CO structure as starting point and replaced either on-top CO or fcc hollow-bonded CO by hydrogen atoms (hcp sites are energetically very similar to fcc; difference 30 meV for CO [54] and 60 meV for H [64]). The stability of the adsorbed hydrogen atoms was determined thereafter. While on-top adsorbed hydrogen with co-adsorbed hollow-bonded CO is endothermic by 184 meV, H in a threefold hollow site with co-adsorbed on-top CO has an exothermic adsorption energy of 0.4 eV. We conclude that CO initially occupies on-top sites while H atoms are, after the dissociative adsorption of the molecule, adsorbed in threefold hollow sites. Although the adsorption energy of on-top

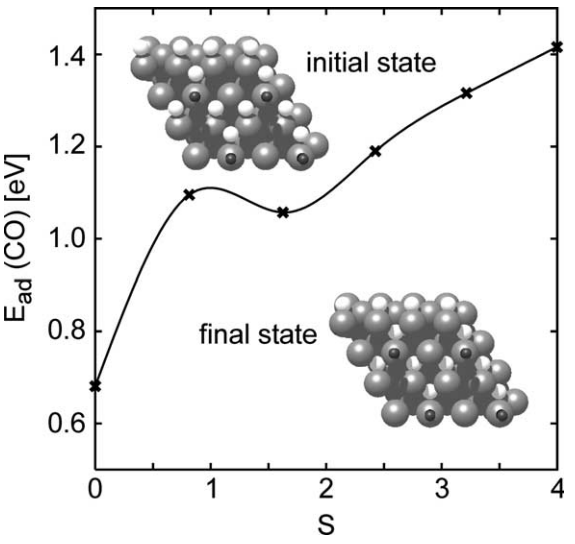

Fig. 4. On-top CO adsorption energy upon vertical (subsurface) diffusion of hydrogen atoms (*s* is the reaction coordinate). The configurations of the two end-points of the reaction path are also shown.

CO is reduced in the presence of hydrogen (Fig. 4, "initial state"), this structure is stable which seems to be in conflict with the observed "destabilization" of on-top CO. However, as shown below, the high mobility of hydrogen must also be taken into account.

Regarding vertical hydrogen diffusion, i.e. the transition from surface to subsurface sites, the diffusion barrier in the presence of coadsorbed CO is only half of that on clean Pd(1 1 1) (0.22 eV as compared to 0.40 eV, respectively). Fig. 4 shows the CO adsorption energy on a neighboring on-top site along the reaction (H subsurface diffusion) pathway. The CO adsorption energy increases monotonously along the reaction pathway and vertical hydrogen diffusion has therefore not the potential to "throw off" on-top CO molecules. This result agrees with our experiments showing that on-top CO was stable even in the presence of subsurface and bulk hydrogen (cf. Figs. 1(d) and 3(c)).

The picture changes when the horizontal (surface) diffusion of a H atom near on-top CO is taken into account. The total adsorption energy of an on-top CO molecule and a hydrogen atom in a neighboring fcc hollow site is 1.68 eV. This is 0.28 eV less than the sum of an isolated CO molecule

and an isolated H atom (illustrating the repulsive interaction), i.e. it takes 0.28 eV for a hydrogen atom far away from CO to approach the other species. Moving the hydrogen atom to the adjacent bridge site without allowing the CO molecule to leave the on-top site costs an additional energy of 0.23 eV and, furthermore, the forces on the CO molecule make this an unstable configuration. However, an energy of 0.62 eV is *gained* if the fcc hydrogen atom moves to the adjacent bridge site and the on-top CO molecule is pushed to the bridge site furthest away from the hydrogen atom. This hydrogen-induced shift of CO from on-top to bridge is even more favorable than the same transition without coadsorbed hydrogen (which yields only 0.41 eV). This explains the absence of on-top CO, but only if this interaction is passed on from the domain boundaries of neighboring CO and H islands to inner sections of the CO domains. As mentioned, such an effect is possible and was observed by STM for the CO–H/Pd(1 1 1) system [18,19].

We have also investigated the effect of coadsorbed hydrogen by calculating vibrational frequencies (Fig. 5). First, stretching frequencies of (pure) CO were calculated at 0.33 ML coverage for each species and compared to those observed by SFG. The calculated values in the harmonic approximation (Fig. 5(a), (c) and (d)) are 2063 cm^{-1} for on-top CO, 1899 cm^{-1} for bridge bonded CO and 1827 and 1825 cm^{-1} for fcc and hcp hollow bonded CO, respectively [54], in good agreement with [49,50]. Experimentally, on-top CO vibrates at ~2090 cm^{-1} (≈0.15 ML on-top CO as part of the 0.63 ML $(4\sqrt{3} \times 8)$rect structure; cf. Figs. 1(d), 6 and 2 of Ref. [1]), bridge-bonded CO has a resonance at ~1920 cm^{-1} (at ~0.5 ML; Fig. 2 of Ref. [1]) and hollow-bonded CO lies at ~1850 cm^{-1} (at 0.33 ML; cf. Fig. 1 of Ref. [2]). In all cases the calculated value is about 20–25 cm^{-1} lower than the experimental one and can be matched by a scaling factor of 1.012 (Fig. 5).

Second, the frequency of bridge bonded CO *with a hydrogen atom in the neighboring bridge site*, i.e. the transition state of H diffusing next to initially top-adsorbed CO (Fig. 5(b)), was calculated. A value of 1883 cm^{-1}, i.e. 16 cm^{-1} lower than the calculated value of bridge-adsorbed CO on the clean surface (1899 cm^{-1}), was obtained. Hydrogen donates an electron to the Pd substrate which results in an increased backdonation between Pd and CO. According to the Blyholder model (its validity was supported by a first-principles study of CO on Pt(1 1 1) [82]), this weakens the C–O bond and thus shifts the CO frequency to lower energy (such substrate-mediated interactions also occur when CO is co-adsorbed with alkali metals [83]). Consequently, bridge bonded CO with a neighboring hydrogen atom should lead to experimental frequencies of—depending on the bridging CO coverage—about 1905 cm^{-1} ($\theta_{CO} = 0.5$ ML) or about 1950 cm^{-1} ($\theta_{CO} = 0.63$ ML).

Even though bridge bonded CO at 1948 cm^{-1} (Fig. 1(e)) and weak features around 1900 cm^{-1}

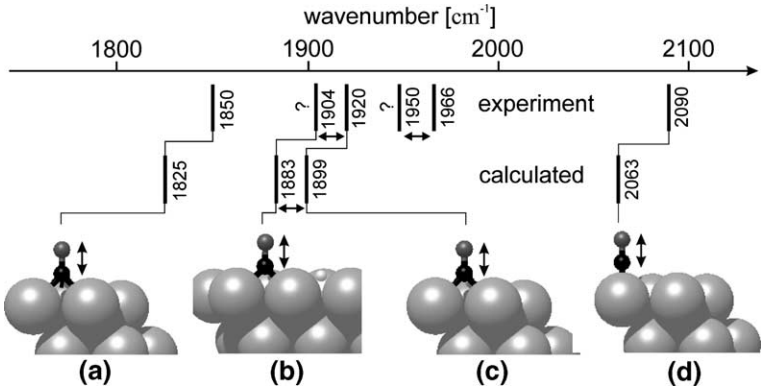

Fig. 5. Calculated and experimental CO stretching frequencies for different configurations: (a) hollow-bonded CO, (b) bridge-bonded CO with neighboring hydrogen, (c) bridge-bonded CO and (d) on-top CO.

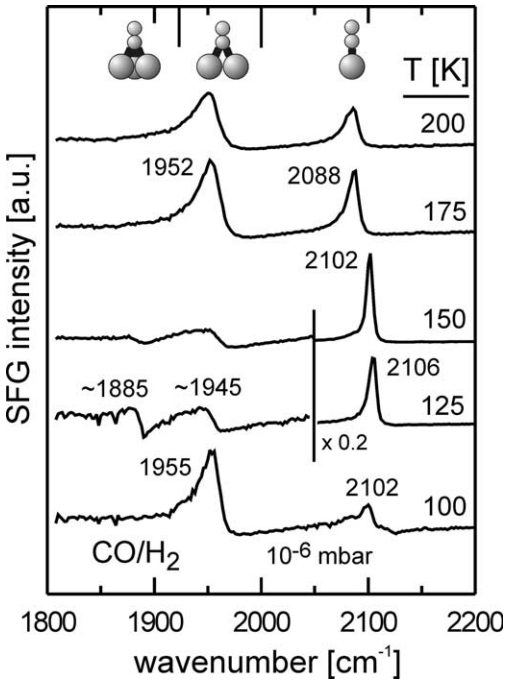

Fig. 6. SFG spectra acquired during exposure of Pd(1 1 1) to 10^{-6} mbar CO/H_2 mixture (1:1) between 100 and 200 K.

(Ref. [22]) were in fact experimentally observed after co-dosing CO and H_2, an *unambiguous* identification of a H-induced shift is difficult for several reasons. First, since the frequency of bridge bonded CO is strongly coverage dependent (e.g. changing about 45 cm^{-1} between 0.5 and 0.65 ML [2,22]), an observed shift may also originate from coverage changes. In fact, the bridge bonded CO frequency observed after adsorbing CO/H_2 mixtures (1948 cm^{-1}; Fig. 1(e)) is very similar to that of pure CO layers around 0.55 ML coverage. Second, the H-induced shift should only affect CO molecules in the immediate vicinity of H atoms, i.e. only bridge bonded CO at the domain boundaries. Since the abundance of this species is much smaller than that of "regular" bridge bonded CO within the CO islands, it may not be easily detected by SFG. IRAS (exhibiting higher resolution than SFG) may be able to better differentiate between these two species.

In any case, experimental and theoretical results agree in showing that on-top CO is unstable when hydrogen diffuses on a Pd(1 1 1) surface while the vibrational peak of bridge-adsorbed CO is (slightly) shifted. Quantitative theoretical calculations regarding hydrogen diffusion at higher CO coverages would require much larger supercells than the p(2×2) cell of our previous calculation for two reasons: First, in tightly packed adsorbate layers the shift of a single adsorbate affects a large number of neighbors, second, the limitation of the CO coverage to ~0.55 ML CO by coadsorbed H could only be simulated in huge supercells.

We have performed several molecular dynamics (MD) simulations in (2×2) Pd(1 1 1) supercells with an initial (2×2)-3CO ordered structure and several hydrogen atoms in the cell. In all runs the on-top CO desorbed/shifted when hydrogen atoms passed while hollow-adsorbed CO molecules adapted to neighboring H atoms. These results qualitatively corroborate the conclusion that diffusing hydrogen destabilizes on-top adsorbed CO molecules, leading to the disappearance of the characteristic high frequency peak in the vibrational SFG spectrum.

In the preceding section (CO adsorption on H-precovered surfaces) it was shown that the site blocking of hydrogen vanished at 150 K (Fig. 1(d)). Similarly, when 10 L of a CO/H_2 *mixture* were dosed at 150 K, an SFG spectrum was observed with a bridge peak at 1958 cm^{-1} and an on-top peak at 2090 cm^{-1} indicating a CO coverage of ~0.65 ML (Fig. 1(f)). In contrast to the corresponding measurement at 100 K (Fig. 1(e)), the on-top site was now clearly populated. Apparently, hydrogen was no longer able to hinder CO adsorption on on-top sites. The structure is identical to that of a pure CO exposure and also TDS did not show indications of any surface hydrogen, again suggesting that H had moved to the Pd bulk.

3.5. Hydrogen bulk dissolution

In Sections 3.3 and 3.4 we have shown that at 100 K hydrogen remained on the surface and either completely prevented CO adsorption or destabilized on-top CO and limited the CO coverage to ~0.55 ML. At 150 K, surface hydrogen was replaced by CO, finally leading to pure CO layers. Apparently, the site blocking effect of H

vanished at a temperature between 100 and 150 K, as the onset-temperature of hydrogen diffusion into the Pd bulk is reached. In order to determine this temperature we have exposed Pd(1 1 1) to 10^{-6} mbar CO/H_2 at increasing temperature (Fig. 6). When (part of) the hydrogen atoms leave the surface, the CO islands are no longer restricted to the 0.5 ML c(4×2) structure and reorganize to the 0.75 ML (2×2) structure (due to further CO adsorption from the gas phase). Since this produces a large on-top CO peak, the transition should be detectable by SFG. As discussed above, the presence of coadsorbed CO may further promote H bulk dissolution, because it reduces the H diffusion barrier between surface and subsurface sites by about 50%.

Upon exposing 10^{-6} mbar CO/H_2 at 100 K (Fig. 6), a small on-top signal appeared beside a bridge peak at 1955 cm^{-1}, but the on-top intensity was only ~5% of that in a "normal" 0.75 ML CO structure [2,22], thus indicating that H destabilized on-top CO. Subsequently, the temperature was raised stepwise to 200 K, keeping the 10^{-6} mbar CO/H_2 background pressure. At 125 K a strong on-top peak occurred and the SFG spectrum was typical of a (2×2) saturation structure with bands at 1885 and 2106 cm^{-1} (fcc and hcp hollow and on-top CO), and with some contribution of domains with 0.63 ML structure (~1945 cm^{-1}), as described in detail in Ref. [22]. At 150 K the hollow and bridge band decreased and at 175 and 200 K spectra typical of ~0.65 ML (bridge/on-top) CO were obtained. The spectra at 125 K and above show no indications of a site blocking by H, i.e. at these temperatures hydrogen already moves into the Pd bulk. Because the H site blocking is also manifest by restricting the CO coverage to ~0.55 ML, CO-TDS can also be used to determine the onset of hydrogen bulk diffusion. By adsorbing 10 L CO/H_2 between 90 and 150 K (in increments of 10°) and subsequently measuring the CO coverage by TDS, an onset temperature of ~125 K was again observed.

The diffusion of surface hydrogen into the Pd bulk and thus the disappearance of a direct CO–H interaction were also examined by theoretical calculations (not including the promoting effect of CO). Three possibilities were considered and quantitatively estimated based on DFT: (i) thermodynamic (entropy driven) solution of hydrogen in the bulk instead of adsorption in subsurface sites, (ii) a thermodynamic phase change from ordered palladium hydride in the surface region to a disordered Pd hydride dissolved in the bulk (lattice gas model), and (iii) kinetically driven diffusion of hydrogen away from the surface. These three approaches are discussed in the following.

(i) Entropy driven solution of hydrogen in the bulk instead of adsorption in subsurface sites: The adsorption energy in subsurface sites is around 0.28 eV (0.25 ML coverage) both in tetragonal and octahedral sites at a Pd_4H occupation in the subsurface layer, decreasing by only 10 meV for a full layer of tetrahedral subsurface hydrogen. The bulk solvation energy is 0.13 eV in $Pd_{64}H$ stoichiometry (all adsorption energies are with respect to $\frac{1}{2} * E_{H_2}$). We calculated the free energy per adsorbate N

$$F/N = E_{ad} - TS/N \tag{1}$$

for both subsurface adsorbed (ss) and bulk dissolved (bd) hydrogen under the assumptions of zero entropy for subsurface hydrogen ($S_{ss} = 0$) and 10^5 layers of bulk. With n being the number of subsurface sites and $b = 10^5 n$ the total number of sites, we get for the configurational entropy of n hydrogen atoms (full subsurface layer, $N = n$) distributed on b sites

$$S_b = k \ln(b!/(n!(b-n)!)) \approx nk \ln(b/n). \tag{2}$$

So we get from Eq. (1)

$$(F/N)_{ss} = -0.28 \text{ eV} \tag{3a}$$

and

$$(F/N)_{bd} = -0.13 \text{ eV} - T9.921 \times 10^{-4} \text{ eV} \tag{3b}$$

and for $(F/N)_{ss} = (F/N)_{bd}$ an entropy driven phase transition temperature of 151 K.

(ii) Lattice gas model of palladium hydride: The critical temperature of the Ising model in the Bragg Williams approximation is

$$T_c = z\varepsilon/k \tag{4}$$

with z being the coordination number, ε the (spin) interaction energy, and k the Boltzmann factor. In the lattice gas model the interaction energy has to

be replaced by $\varepsilon_0/4$, ε_0 being the interaction energy of nearest neighbors. We determined the formation energy of palladium hydride by calculating the hydrogen solution energy for different hydrogen concentrations, the "low concentration limit" being a $Pd_{64}H$ cell. The energy difference with respect to the low concentration limit provides the value of $z\varepsilon_0$. The maximum energy is achieved for a Pd_4H hydride with $z\varepsilon_0/4 = 0.01$ eV. A similar value was previously obtained applying the effective medium theory [84], although in those calculations the solution energy increases slightly up to a Pd:H ratio of 1, in contrast to our results. The critical temperature according to our calculations is 116 K.

(iii) Kinetically driven diffusion of hydrogen away from the surface: We have calculated several diffusion barriers starting from a full monolayer of hydrogen on the surface. The diffusion barrier from an fcc threefold hollow surface adsorption site to a subsurface octahedral site is 0.48 eV. The diffusion in the subsurface layer from octahedral to tetrahedral sites and back has diffusion barriers of 0.13 and 0.16 eV, respectively. The diffusion from subsurface to bulk sites has an activation energy of 0.22 eV when starting from tetrahedral subsurface sites and 0.25 eV when starting from octahedral sites. Assuming a prefactor of 10^{13} s^{-1} we list the temperatures that lead to a rate of 5×10^{-3} s^{-1}, i.e. the diffusion of all atoms in the initial sites in 200 s (which is approximately the time scale of our TPD experiments): surface–subsurface: 157 K; inter–subsurface: 42 and 52 K, respectively; subsurface–bulk: 72 and 82 K, respectively.

From a kinetic point of view it seems at first hand unlikely that a considerable amount of hydrogen adsorbed in threefold hollow positions moves subsurface through the *close-packed* surface at 90–100 K. However, this does not contradict experimental observations of subsurface H at these temperatures (e.g. [13,62]) because hydrogen may reach subsurface sites through defects or steps, whereupon it diffuses easily within the subsurface layer. Below the surface layer, diffusion rates at around 100 K are already high enough to reach thermodynamic equilibrium in a near-surface region in reasonable time. On the other hand, although kinetically possible, at temperatures lower than 120–150 K subsurface as well as other near-surface hydrogen has still no strong intention to dissolve in the Pd bulk because of (a) the energetic favor of subsurface sites as compared to bulk sites and (b) the interaction energy of close hydrogen atoms in the bulk forming a hydride. Only above that temperature range the entropy gain through solution surpasses the energetic disadvantages and hydrogen dissolves in the bulk.

Summarizing, the three models suggest a temperature range of 120–150 K for bulk H dissolution which reasonably agrees with our experimentally observed value. As mentioned, the promoting effect of CO or any other coadsorbed molecule was not considered in the calculations. For coadsorbed oxygen Mitsui et al. [19] observed by STM that hydrogen disappeared from Pd(1 1 1) upon heating to ~200 K, as evident from the reversal of the hydrogen-induced compression of an oxygen layer (which relaxed from a $(\sqrt{3}\times\sqrt{3})$ to a (2×2) structure). Since no hydrogen desorbs at this temperature, this observation can only be explained if hydrogen moved to subsurface or deeper sites.

For completeness we want to mention that the spectra in Fig. 6 are, of course, not reversible. After heating to 200 K (which distributes H in the Pd crystal), upon cooling back to 90 K the CO layer prevents H adsorption from the gas phase and also a re-agglomeration of bulk H in the surface region does not occur. Previously calculated diffusion barriers for H in Pd bulk are around 0.2 eV, in good agreement with experiments [85]. This leads to a diffusion rate of about 60 s^{-1} at 90 K (again assuming a prefactor of 10^{13} s^{-1}) or a time of 2×10^7 s until the average displacement of a particle $\Delta z = \sqrt{(2Dt)}$ is 5×10^4 (i.e. until H reaches the surface).

3.6. Implications on hydrogenation reactions

How do the described effects influence studies of hydrogenation reactions on single crystals? The strong site blocking ability of CO is well-established and manifest as reduced reaction rate under CO-rich conditions (negative CO reaction order

[86,87]). Hydrogen is able to prevent CO adsorption or, at least, CO adsorption at on-top sites below ~125 K, but at higher temperature CO replaces surface H which moves to subsurface and bulk sites. CO may in fact promote H dissolution by reducing the H subsurface diffusion activation barrier or, as suggested by Eriksson and Ekedahl [14], by temporarily increasing the local hydrogen surface concentration.

Consequently, CO and H cannot readily react because under most conditions studied they do not coexist on the surface. Another implication from the CO-assisted hydrogen dissolution is that thermal desorption spectra of the CO–H system can be quite misleading. Even when H coexists with CO on Pd(1 1 1) at 100 K (Fig. 1(e)), H moves to the Pd bulk *during* the TPD run and finally desorbs around 375 K (similar to Fig. 3(c)). In this case, the H_2-desorption temperature is not characteristic for the initial coadsorbate structure at 100 K.

It is now interesting to ask if coadsorption of H with other molecules (e.g. C_2H_4 or oxygen) exhibits a related behavior or not. TPD spectra of ethylene (C_2H_4) and H_2 adsorption and coadsorption on Pd(1 1 1) are shown in Fig. 3(e)–(h). Desorption spectra of the individual components are presented in Fig. 3(e) and (f), for reference. Although vibrational and photoelectron spectroscopy of C_2H_4 adsorption at ~100 K indicate di-σ bonded ethylene as stable species (e.g. [88–91]), theoretical studies rather suggest a combination of di-σ bonded C_2H_4 at bridge sites and π-bonded C_2H_4 at on-top sites as surface species [92,93]. TDS spectra of C_2H_4 adsorption (Fig. 3(f)) show a broad peak with a maximum at 260 K and a small desorption feature at 195 K. While the first can be attributed to di-σ-bonded ethylene, the origin of the low temperature desorption is not clear. It may be due to π-bonded ethylene but may also originate from rearrangements in a purely di-σ bonded ethylene layer, similar to the sharp low-temperature desorption features (~170 K) observed for structural transitions of high-coverage CO layers (hollow/on-top to bridge/on-top transition [23,41]).

Similar to CO, preadsorbed C_2H_4 prevents H adsorption and 1 L hydrogen was thus adsorbed before 1 L C_2H_4 was dosed at 95 K (Fig. 3(g) and (h)). In contrast to CO, C_2H_4 is able to adsorb on a H-precovered surface (Fig. 3(h)) at 95 K but C_2H_4 is now (mainly) bonded in a π-configuration which desorbs at lower temperature (this has also been observed by IRAS [89,94]). The difference between CO and C_2H_4 is presumably related to the preferred adsorption sites of the two molecules. Preadsorbed H occupies threefold hollow sites and thus blocks the most stable CO adsorption site while π-bonded C_2H_4 can still adsorb on on-top sites (while di-σ-bonded ethylene is (partly) blocked). The change in the C_2H_4 adsorption configuration demonstrates that C_2H_4 and H coexist on the surface at 95 K.

Based on the calculations in Section 3.5, H bulk dissolution should also occur during TPD of the H/C_2H_4 system between ~125 and 200 K. This leads to a reduction of the surface H concentration and to a (partial) separation of H (in the bulk) and C_2H_4 (on the surface), similar to the CO–H case, which decreases the probability of a catalytic reaction. In fact, for C_2H_4 hydrogenation on Pd(1 1 1) Stacchiola et al. [89] and Doyle et al. [95] observed only very small amounts of ethane (less than a few percent) by TPD. At temperatures when H "returns" to the surface (and desorbs recombinatively at ~300 K; Fig. 3(g)), C_2H_4 has already mostly desorbed. Since there is no stable adsorbate layer left which could shift hydrogen desorption to higher temperature, H_2 desorbs at its "regular" temperature around 300 K. A small amount of ethylene decomposes into ethylidyne C_2H_3 around 300 K [91,96–99] and its further decomposition leads to the small H_2 peak at ~425 K (Fig. 3(g)).

In the oxygen/hydrogen coadsorption experiments by Mitsui et al. [19] hydrogen disappeared from Pd(1 1 1) upon heating to ~200 K (and the oxygen islands relaxed from a $(\sqrt{3}\times\sqrt{3})$ to a (2×2) structure). The higher temperature of H bulk dissolution may be related to a different promotion by oxygen. Hydrogen reappeared on the surface above 220 K, most likely through the clean Pd areas between the oxygen islands, and reacted away the oxygen [19]. It is not clear if a complete oxygen layer on Pd(1 1 1) (not desorbing below 800 K) would have increased the hydrogen desorption temperature (similar to CO) or would have simply been reacted away.

Finally, one should note that the coadsorption behavior and reactivity of the described molecules is again different on Pd nanoparticles. In contrast to Pd(1 1 1), on oxide supported Pd nanoparticles catalytic CO hydrogenation can be successfully performed both under low- [100] and high-pressure conditions [6,101–104]. Pd nanoparticles exhibit facets other than (1 1 1) and step-, edge- and corner sites which may reduce site blocking effects and provide new geometries for CO–H interaction [1,2,105]. Another difference is related to the bonding of hydrogen. TPD experiments [95,96] have shown that, in contrast to Pd(1 1 1), hydrogenation of C_2H_4 and various pentenes readily occurred on ~5 nm Pd nanoparticles supported by Al_2O_3, due to an enhanced accessibility of (subsurface) H on Pd nanoparticles. The enhanced H accessibility on Pd nanoparticles shows up in TPD as weakly bonded hydrogen states (desorbing between 200 and 280 K), and originates from the reduced diffusion length of bulk H which is confined to the dimensions of a nanometer-sized Pd particle. On Pd(1 1 1), H can dissolve in the bulk during the TPD run and, therefore, the surface H required for C_2H_4 hydrogenation seems to be only available at mbar pressures, when a dynamic equilibrium between adsorbed and gas phase hydrogen is established [2,90]. Combined SFG-TPD coadsorption studies of CO–H interaction on Pd–Al_2O_3 are currently performed.

4. Conclusions

Non-linear optical sum frequency generation (SFG) vibrational spectroscopy was combined with density functional theory (DFT) to study adsorbate–adsorbate interactions of CO and H on Pd(1 1 1). The resulting coadsorbate structures were mainly determined by the mutual site blocking of CO and H and by H bulk dissolution, which both depend on the type of gas exposure (sequential vs. co-dosing) and the exposure temperature. The results can be summarized as follows:

(a) Dissociative hydrogen adsorption did not occur on CO-precovered Pd(1 1 1) for CO coverages between 0.75 and 0.33 ML. Purely steric arguments cannot explain the observed site blocking but DFT calculations determined an activation barrier of at least 2.5 eV which renders H adsorption on a CO-precovered surface very unlikely.

(b) No CO adsorption was observed on hydrogen-precovered Pd(1 1 1) at 100 K and also DFT indicated an unstable CO adsorption configuration under these conditions. In contrast, at 150 K CO was able to replace preadsorbed surface hydrogen which moved to Pd bulk sites.

(c) When a 1:1 CO/H_2 mixture was adsorbed on Pd(1 1 1), the adsorbate structure again strongly depended on temperature. Below ~125 K separate CO and H islands were produced but on-top CO was strongly suppressed and the CO coverage was limited to ~0.55 ML. DFT calculations identified surface H diffusion to be responsible for the absence of on-top CO. In fact, an energy of 0.62 eV is gained when a hydrogen atom moves between two hollow sites via an adjacent bridge site and an on-top CO molecule is pushed to the bridge site furthest away from the hydrogen atom. The stretching frequency of CO in a bridge site with a hydrogen atom in the neighboring bridge site (transition state of diffusing H) was calculated to be 16 cm^{-1} lower than bridge-adsorbed CO on the clean surface. When adsorbing a CO/H_2 mixture above ~125 K, CO was able to replace surface hydrogen which moved to Pd subsurface/bulk sites and adsorbate structures identical to those of pure CO exposure were obtained.

(d) The onset-temperature of hydrogen diffusion into the Pd bulk was studied both experimentally and theoretically. SFG spectra of CO/H_2 mixtures indicated that around 125 K H bulk diffusion occurred and pure CO surface layers were observed. Hydrogen diffusion into the Pd bulk was examined by theoretical calculations using various approaches (entropy driven solution of hydrogen in the bulk; thermodynamic phase change from an ordered to a disordered palladium hydride; kinetically driven hydrogen diffusion) yielding onset-temperatures of 120–150 K. The presence of coadsorbed CO reduces the H diffusion barrier between surface and subsurface sites by about 50% and thus promotes H bulk dissolution.

(e) A comparison with the C_2H_4/H coadsorption system has shown a reduced site blocking ability of hollow-bonded H towards C_2H_4 at 100 K, which can be explained by the different preferred/accessible adsorption sites of CO and C_2H_4 on Pd(1 1 1). Hydrogen bulk diffusion during temperature programmed desorption may explain the small amount of C_2H_4 hydrogenation.

(f) The strong dependence of coadsorbate structures on the type of gas exposure (sequential vs. mixture), on the adsorption temperature and, of course, on the type of molecules (governing the adsorption geometry and binding energy) and their relative abundance makes predictions of the diverse behavior of coadsorbate structures very difficult.

Acknowledgements

This work was supported by the Priority Program SPP 1091 of the German Science Foundation (DFG) and by the Austrian Science Fund (FWF) within the research project "Gas–Surface Interactions" (S8106). Helpful discussions with A. Eichler and T. Klüner are gratefully acknowledged.

References

[1] H. Unterhalt, G. Rupprechter, H.-J. Freund, J. Phys. Chem. B. 106 (2002) 356.
[2] G. Rupprechter, H. Unterhalt, M. Morkel, P. Galletto, L. Hu, H.-J. Freund, Surf. Sci. 502–503 (2002) 109.
[3] K. Christmann, Surf. Sci. Rep. 9 (1988) 1.
[4] K. Christmann, Prog. Surf. Sci. 48 (1995) 15.
[5] C. Chinchen, P.J. Denny, J.R. Jennings, M.S. Spencer, K.C. Waugh, Appl. Catal. 36 (1988) 1.
[6] A.F. Gusovius, T.C. Watling, R. Prins, Appl. Catal. A 188 (1999) 187.
[7] H. Conrad, G. Ertl, E.E. Latta, J. Catal. 35 (1974) 363.
[8] R.J. Behm, V. Penka, M.-G. Cattania, K. Christmann, G. Ertl, J. Chem. Phys. 78 (1983) 7486.
[9] G.A. Kok, A. Noordermeer, B.E. Nieuwenhuys, Surf. Sci. 135 (1983) 65.
[10] H. Conrad, G. Ertl, E.E. Latta, Surf. Sci. 41 (1974) 435.
[11] K.H. Rieder, W. Stocker, Surf. Sci. 148 (1984) 139.
[12] S. Wilke, D. Henning, R. Löber, M. Methfessel, M. Scheffler, Surf. Sci. 307–309 (1994) 76.
[13] H. Okuyama, W. Siga, N. Takagi, M. Nishijima, T. Aruga, Surf. Sci. 401 (1998) 344.
[14] M. Eriksson, L.-G. Ekedahl, Appl. Surf. Sci. 133 (1998) 89.
[15] C. Nyberg, L. Westerlund, Surf. Sci. 256 (1991) 9.
[16] A.D. Johnson, K.J. Maynard, S.P. Daley, Q.Y. Yang, S.T. Ceyer, Phys. Rev. Lett. 67 (1991) 927.
[17] G. Rupprechter, G.A. Somorjai, Catal. Lett. 48 (1997) 17.
[18] M.K. Rose, T. Mitsui, J. Dunphy, A. Borg, D.F. Ogletree, M. Salmeron, P. Sautet, Surf. Sci. 512 (2002) 48.
[19] T. Mitsui, M.K. Rose, E. Fomin, D.F. Ogletree, M. Salmeron, Surf. Sci. 511 (2002) 259.
[20] T. Mitsui, M.K. Rose, E. Fomin, D.F. Ogletree, M. Salmeron, Nature 422 (2003) 705.
[21] T. Mitsui, M.K. Rose, E. Fomin, D.F. Ogletree, M. Salmeron, Surf. Sci. 540 (2003) 5.
[22] M. Morkel, H. Unterhalt, M. Salmeron, G. Rupprechter, H.-J. Freund, Surf. Sci. 532–535 (2003) 103.
[23] M. Morkel, G. Rupprechter, H.-J. Freund, J. Chem. Phys. 119 (2003) 10853.
[24] G. Rupprechter, T. Dellwig, H. Unterhalt, H.-J. Freund, Top. Catal. 15 (2001) 19.
[25] G. Rupprechter, Phys. Chem. Chem. Phys. 3 (2001) 4621.
[26] G. Kresse, J. Furthmüller, Phys. Rev. B 54 (1996) 11169.
[27] G. Kresse, J. Hafner, Phys. Rev. B 47 (1993) 558.
[28] J.P. Perdew, Y. Wang, Phys. Rev. B (1992) 13244.
[29] B. Hammer, L.B. Hansen, J.K. Nørskov, Phys. Rev. B 59 (1999) 7413.
[30] H.J. Monkhorst, J.D. Pack, Phys. Rev. B 13 (1976) 5188.
[31] P.E. Blöchl, Phys. Rev. B 50 (1994) 17953.
[32] G. Kresse, D. Joubert, Phys. Rev. B 59 (1999) 1758.
[33] R.P. Feynman, Phys. Rev. B 56 (1939) 340.
[34] X. Guo, J.T. Yates, J. Chem. Phys. 90 (1989) 6761.
[35] J. Szanyi, W.K. Kuhn, D.W. Goodman, J. Vac. Sci. Technol. A 11 (1993) 1969.
[36] M. Beutl, J. Lesnik, Vacuum 61 (2001) 113.
[37] H. Ohtani, M.A. Van Hove, G.A. Somorjai, Surf. Sci. 187 (1987) 372.
[38] I. Zasada, M.A. van Hove, Surf. Sci. Lett. 457 (2000) L421.
[39] A.M. Bradshaw, F.M. Hoffmann, Surf. Sci. 72 (1978) 513.
[40] F.M. Hoffmann, Surf. Sci. Rep. 3 (1983) 103.
[41] W.K. Kuhn, J. Szanyi, D.W. Goodman, Surf. Sci. Lett. 274 (1992) L611.
[42] P. Sautet, M.K. Rose, J.C. Dunphy, S. Behler, M. Salmeron, Surf. Sci. 453 (2000) 25.
[43] S. Surnev, M. Sock, M.G. Ramsey, F.P. Netzer, M. Wiklund, M. Borg, J.N. Andersen, Surf. Sci. 470 (2000) 171.
[44] V.V. Kaichev, I.P. Prosvirin, V.I. Bukhtiyarov, H. Unterhalt, G. Rupprechter, H.-J. Freund, J. Phys. Chem. B. 107 (2003) 3522.
[45] B. Bourguignon, S. Carrez, B. Dragnea, H. Dubost, Surf. Sci. 418 (1998) 171.
[46] G. Rupprechter, H. Unterhalt, M. Morkel, P. Galletto, T. Dellwig, H.-J. Freund, Vacuum 71 (2003) 83.
[47] M. Tüshaus, W. Berndt, H. Conrad, A.M. Bradshaw, B. Persson, Appl. Phys. A 51 (1990) 91.
[48] T. Gießel et al., Surf. Sci. 406 (1998) 90.

[49] D. Loffreda, D. Simon, P. Sautet, Surf. Sci. 425 (1999) 68.
[50] K. Honkala, P. Pirilä, K. Laasonen, Surf. Sci. 489 (2001) 72.
[51] B. Hammer, Y. Morikawa, J.K. Nørskov, Phys. Rev. Lett. 76 (1996) 2141.
[52] P.J. Feibelman, B. Hammer, J.K. Norskov, F. Wagner, M. Scheffler, R. Stumpf, R. Watwe, J. Dumesic, J. Phys. Chem. B 105 (2001) 4018.
[53] G. Kresse, A. Gil, P. Sautet, Phys. Rev. B 68 (2003) 073401.
[54] R. Hirschl, J. Hafner, Surf. Sci. 498 (2002) 37.
[55] H. Conrad, G. Ertl, J. Koch, E.E. Latta, Surf. Sci. 43 (1974) 462.
[56] I.V. Yudanov, R. Sahnoun, K.M. Neyman, N. Rösch, J. Chem. Phys. 117 (2002) 9887.
[57] I.V. Yudanov et al., J. Phys. Chem. B 107 (2003) 255.
[58] T. Klüner, N. Govind, Y.A. Wang, E.A. Carter, Phys. Rev. Lett. 86 (2001) 5954.
[59] T. Klüner, N. Govind, Y.A. Wang, E.A. Carter, J. Chem. Phys. 116 (2001) 42.
[60] C. Nyberg, L. Westerlund, L. Jönsson, S. Andersson, J. Electron. Spectr. Rel. Phenom. 54/55 (1990) 639.
[61] G.E. Gdowski, T.E. Felter, R.H. Stulen, Surf. Sci. 181 (1987) L147.
[62] T.E. Felter, E.C. Sowa, M.A. Van Howe, Phys. Rev. B 40 (1989) 891.
[63] W. Dong, J. Hafner, Phys. Rev. B 56 (1997) 15396.
[64] W. Dong, V. Ledentu, P. Sautet, A. Eichler, J. Hafner, Surf. Sci. 411 (1998) 123.
[65] J.F. Paul, P. Sautet, Phys. Rev. B 53 (1996) 8015.
[66] G. Mills, H. Jónsson, G.K. Schenter, Surf. Sci. 324 (1995) 305.
[67] D.L. Lynch, S.W. Rick, M.A. Gomez, B.W. Spath, J.D. Doll, L.R. Pratt, J. Chem. Phys. 97 (1992) 5177.
[68] G. Pauer, A. Eichler, M. Sock, M.G. Ramsey, F. Netzer, A. Winkler, J. Chem. Phys. 119 (2003) 1.
[69] S. Holloway, Surf. Sci. 540 (2003) 1.
[70] J.M. White, S. Akther, CRC Critical Rev. Solid State Mater. Sci. 14 (1988) 131.
[71] F.H. Ribeiro, C.A. Gerken, G. Rupprechter, G.A. Somorjai, C.S. Kellner, G.W. Coulston, L.E. Manzer, L. Abrams, J. Catal. 176 (1998) 352.
[72] A. Groß, Appl. Phys. A 67 (1998) 627.
[73] P.A. Gravil, H. Toulhoat, Surf. Sci. 430 (1999) 176.
[74] H.P. Bonzel, H.J. Krebs, Surf. Sci. 117 (1982) 639.
[75] J.K. Norskov, S. Holloway, N.D. Lang, Surf. Sci. 137 (1984) 65.
[76] J. Lauterbach, M. Schick, W.H. Weinberg, J. Vac. Sci. Technol. A 14 (1996) 1511.
[77] M. Wilde, M. Matsumoto, K. Fukutani, T. Aruga, Surf. Sci. 482 (2001) 346.
[78] D. Hoge, M. Tüshaus, A.M. Bradshaw, Surf. Sci. 207 (1988) L935.
[79] H. Wang, R.G. Tobin, D.K. Lambert, G.B. Fisher, C.L. DiMaggio, Surf. Sci. 330 (1995) 173.
[80] R. Zenobi, J. Xu, J.T. Yates, Surf. Sci. 276 (1992) 241.
[81] S. Andersson, Solid State Commun. 21 (1977) 75.
[82] H. Aizawa, S. Tsuneyuki, Surf. Sci. 399 (1998) L364.
[83] H.P. Bonzel, Surf. Sci. Rep. 8 (1987) 43.
[84] O.B. Christensen, P.D. Ditlevsen, K.W. Jacobsen, P. Stoltze, O.H. Nielsen, J.K. Nørskov, Phys. Rev. B 40 (1989) 1993.
[85] X. Ke, G.J. Kramer, Phys. Rev. B 66 (2002) 184304.
[86] B. Klötzer, W. Unterberger, K. Hayek, Surf. Sci. 532–535 (2003) 142.
[87] K. Hayek, M. Fuchs, B. Klötzer, W. Reichl, G. Rupprechter, Top. Catal. 13 (2000) 55.
[88] N. Sheppard, C. De La Cruz, Adv. Catal. 42 (1998) 181.
[89] D. Stacchiola, S. Azad, L. Burkholder, W.T. Tysoe, J. Phys. Chem. B 105 (2001) 11233.
[90] H.-J. Freund, M. Bäumer, J. Libuda, T. Risse, G. Rupprechter, S. Shaikhutdinov, J. Catal. 216 (2003) 223.
[91] M. Sock, A. Eichler, S. Surnev, J.N. Andersen, B. Klötzer, K. Hayek, M.G. Ramsey, F.P. Netzer, Surf. Sci. 545 (2003) 122.
[92] M. Neurock, R.A. van Santen, J. Phys. Chem. B 104 (2000) 11127.
[93] Q. Ge, M. Neurock, Chem. Phys. Lett. 358 (2002) 377.
[94] D. Stacchiola, L. Burkholder, W.T. Tysoe, Surf. Sci. 511 (2002) 215.
[95] A. Doyle, S. Shaikhutdinov, S.D. Jackson, H.-J. Freund, Angew. Chem. 42 (2003) 5240.
[96] S. Shaikhutdinov, M. Heemeier, M. Bäumer, T. Lear, D. Lennon, R.J. Oldman, S.D. Jackson, H.-J. Freund, J. Catal. 200 (2001) 330.
[97] M. Kaltchev, A.W. Thompson, W.T. Tysoe, Surf. Sci. 391 (1997) 145.
[98] D. Stacchiola, G. Katchev, G. Wu, W.T. Tysoe, Surf. Sci. 470 (2000) L32.
[99] L.L. Kesmodel, J.A. Gates, Surf. Sci. 111 (1981) L747.
[100] M. Rothaemel, H.W. Zanthoff, M. Baerns, Catal. Lett. 28 (1994) 321.
[101] A. Gotti, R. Prins, J. Catal. 175 (1998) 302.
[102] A. Gotti, R. Prins, Catal. Lett. 37 (1996) 143.
[103] G.C. Cabilla, A.L. Bonivardi, M.A. Baltanas, Catal. Lett. 55 (1998) 147.
[104] R.F. Hicks, A.T. Bell, J. Catal. 90 (1984) 205.
[105] T. Dellwig, G. Rupprechter, H. Unterhalt, H.-J. Freund, Phys. Rev. Lett. 85 (2000) 776.